Supercontinuum generation in large mode-area microstructured fibers

G. Genty, T. Ritari, and H. Ludvigsen

Fiber-Optics Group, Department of Electrical and Communications Engineering, Helsinki University of Technology, P.O. Box 3500, FI-02015 HUT, Finland

goery.genty@tkk.fi

Abstract: Supercontinuum generation in large mode-area microstructured fibers is demonstrated by launching into the fiber ns pulses from a passively Q-switched Nd:YAG laser. The special properties of these fibers open the way to compact, single-mode, high-power supercontinuum sources with a low divergence of the output beam. The nonlinear phenomena leading to the formation of the broad spectrum are also described.

OCIS codes: (190.4370) Nonlinear optics, fibers; (190.4380) Nonlinear optics, four-wave mixing; (230.3990) Microstructure devices; (290.5860) Scattering, Raman.

References and links

1. See for instance Nonlinear optics of photonic crystals, Special issue of J. Opt. Soc. Am. B **19**, 1961-2296 (2002) or Supercontinuum generation, Special issue of Appl. Phys. B **77**, 143-376 (2003).
2. T. M. Monro, W. Belardi, K. Furusawa, J. C. Baggett, N. G. R. Broderick, and D. J. Richardson, "Sensing with microstructured optical fibres," Meas. Sci. Technol. **12**, 854-858 (2001).
3. I. Hartl, X. D. Li, C. Chudoba, R. K. Ghanta, T. H. Ko, J. G. Fujimoto, J. K. Ranka, R. S. Windeler, "Ultrahigh-resolution optical coherence tomography using continuum generation in an air silica microstructure optical fiber," Opt. Lett. **26**, 608-610 (2001).
4. P. T. Rakich, H. Sotobayashi, J. T. Gopinath, S. G. Johnson, J. W. Sickler, C. W. Wong, J. D. Joannopoulos, and E. P. Ippen, "Nano-scale photonic crystal microcavity characterization with an all-fiber based 1.2 – 2.0 μm supercontinuum," Opt. Express **13**, 821-825 (2005), http://www.opticsexpress.org/abstract.cfm?URI=OPEX-13-3-821
5. M. Lehtonen, G. Genty, and H. Ludvigsen, "Absorption and transmission spectral measurements of fiber-optic components using supercontinuum radiation", Appl. Phys. B **81**, 231-234 (2005).
6. J. K. Ranka, R. S. Windeler, and A. J. Stentz, "Visible continuum generation in air-silica microstructure optical fibers with anomalous dispersion at 800 nm," Opt. Lett. **25**, 25-27 (2000).
7. S. Coen, A. Hing Lun Chau, R. Leonhardt, J. D. Harvey, J. C. Knight, W. J. Wadsworth, and P. St. J. Russell, "White-light supercontinuum generation with 60-ps pump pulses in a photonic crystal fiber," Opt. Lett. **26**, 1356-1358 (2001).
8. W. J. Wadsworth, N. Joly, J. C. Knight, T. A. Birks, F. Biancalana, and P. St. J. Russell, "Supercontinuum and four-wave mixing with Q-switched pulses in endlessly single-mode photonic crystal fibres," Opt. Express **12**, 299-309 (2004), http://www.opticsexpress.org/abstract.cfm?URI=OPEX-12-2-299
9. J. M. Dudley, L. Provino, N. Grossard, H. Maillotte, R. S. Windeler, B. J. Eggleton, and S. Coen, "Supercontinuum generation in air-silica microstructured fibers with nanosecond and femtosecond pulse pumping," J. Opt. Soc. Am. B **19**, 765-771 (2002).
10. A. K. Abeeluck, C. Headley, and C. G. Jørgensen, "High-power supercontinuum generation in highly nonlinear, dispersion-shifted fibers by use of a continuous-wave Raman fiber laser," Opt. Lett. **29**, 2163-2165 (2004).
11. A. K. Abeeluck and C. Headley, "Supercontinuum growth in a highly nonlinear fiber with a low-coherence semiconductor laser diode," Appl. Phys. Lett. **85**, 4863-4865 (2004).
12. J. C. Knight, T. A. Birks, R. F. Cregan, P. St. J. Russell, and J. P. de Sandro, "Large mode area photonic crystal fibre," Electron. Lett. **34**, 1347-1348 (1998).
13. M. D. Nielsen, C. Jacobsen, N. A. Mortensen, J. R. Folkenberg, and H. R. Simonsen, "Low-loss photonic crystal fibers for transmission systems and their dispersion properties," Opt. Express **12**, 1372-1376 (2004), http://www.opticsexpress.org/abstract.cfm?URI=OPEX-12-7-1372
14. M. D. Nielsen, J. R. Folkenberg, N. A. Mortensen, and A. Bjarklev, "Bandwidth comparison of photonic crystal fibers and conventional single-mode fibers," Opt. Express **12**, 430-435 (2004), http://www.opticsexpress.org/abstract.cfm?URI=OPEX-12-3-430

#8283 - $15.00 USD Received 26 July 2005; Revised 14 September 2005; Accepted 11 October 2005

15. T. Ritari, T. Niemi, M. Wegmuller, N. Gisin, J. R. Folkenberg, A. Pettersson, and H. Ludvigsen, "Polarization-mode dispersion of large mode-area photonic crystal fibers," Opt. Commun. **226**, 233-239 (2003).
16. M. D. Nielsen and N. A. Mortensen, "Photonic crystal fiber design based on the V-parameter," Opt. Express **11**, 2762-2768 (2003), http://www.opticsexpress.org/abstract.cfm?URI=OPEX-11-21-2762
17. D. Yevick and B. Hermansson, "Efficient beam propagation techniques," IEEE J. Quantum Electron. **26**, 109-112 (1990).
18. T. Sylvestre, H. Maillote, E. Lantz, and P. Tchofo Dinda, "Raman-assisted parametric frequency conversion in a normally dispersive single-mode fiber," Opt. Lett. **24**, 1561-1563 (1999).
19. R. H. Stolen, C. Lee, and R. K. Jain, "Development of the stimulated Raman spectrum in single-mode silica fibers," J. Opt. Soc. Am. B **1**, 652-657 (1984).
20. A. K. Abeeluck and C. Headley, "Continuous-wave pumping in the anomalous- and normal-dispersion regimes of nonlinear fibers for supercontinuum generation," Opt. Lett. **30**, 61-63 (2005).
21. N. Bloembergen and Y. R. Shen, "Coupling between vibrations and light waves in Raman laser media," Phys. Rev. Lett. **12**, 504-507 (1964).
22. E.A. Golovchenko, P. V. Mamyshev, A. N. Pilipestskii, and E. M. Dianov, "Mutual influence of the parametric effects ans stimulated Raman scattering in optical fibers," IEEE J. Quantum Electron. 26, 1815-1820 (1990).
23. G. Genty, M. Lehtonen, and H. Ludvigsen, "Effect of cross-phase modulation on supercontinuum generated in microstructured fibers with sub-30 fs pulses," Opt. Express **12**, 4614-4624 (2004), http://www.opticsexpress.org/abstract.cfm?URI=OPEX-12-19-4614

1. Introduction

With the rapid development of microstructured fibers (MFs), supercontinuum (SC) generation has been the focus of intense research over the past years [1]. The interest for this type of ultra-broadband sources originates from the wide range of potential applications in various fields such as sensors, characterization of optical components, interferometry or optical coherence tomography [2-5]. Typically, supercontinua have been generated in short lengths of narrow-core MFs by pumping with femtosecond laser pulses [6] or in several meter-long MFs employing picosecond or nanosecond pulsed sources [7-9]. Lately, SC generation has also been reported in highly nonlinear, dispersion-shifted fibers pumped by continuous wave sources such as cascaded Raman fiber lasers and Raman-amplified laser diodes [10-11]. Narrow-core MFs possess high numerical aperture resulting in a large divergence of the output beam, which requires additional optics in order to couple the SC light into standard fibers or optical components. Furthermore, the dimension of the core on the order of a micron yields a high local intensity and large attenuation at wavelengths larger than the core size, thereby limiting the maximum output power and infrared bandwidth obtainable. Narrow-core MFs may also exhibit multi-mode behavior, which is detrimental to SC applications.

On the other hand, large mode-area microstructured fibers (LMA-MFs) can combine a large core size and a low numerical aperture while still allowing only the fundamental mode to propagate at all wavelengths [12-14]. In addition, the long-wavelength cut-off of LMA-MFs is located at longer wavelengths than in the case of narrow-core MFs. Furthermore, the larger dimensions allow for a better control of the microstructure during the manufacturing process and fibers with almost perfectly symmetrical microstructures, thus eliminating birefringence, have been reported [15]. This may prove to be useful if no polarization dependence of the generated supercontinuum is desired. Moreover, as the absorption of the water peak decreases for larger core dimensions, LMA-MFs exhibit low losses compared to narrow-core MFs at 1390 nm.

In this paper, we investigate the generation of supercontinuum in different LMA-MFs employing a compact, diode-pumped nanosecond laser. This type of source may be particularly useful in applications requiring broadband sources with low numerical aperture where, e.g., a high brightness, large depth of focus or circular beam is needed. Moreover, the relatively large core-size of LMA-MFs allows for direct insertion of a FC/PC output connector or easy splicing to standard single-mode fibers leading the route to fully compact and functional sources.

#8283 - $15.00 USD Received 26 July 2005; Revised 14 September 2005; Accepted 11 October 2005

2. Experiments

The fibers used in the experiments are three large mode-area MFs with a triangular microstructured cladding [15]. The core diameter of the three fibers referred to as LMA-10, LMA-15 and LMA-20, are equal to 10.8, 14.8 and 19.4 μm, respectively. Microscope images of the cross section of LMA-10 and LMA-15 are displayed in Fig. 1. Note that the scaling is different for the two images.

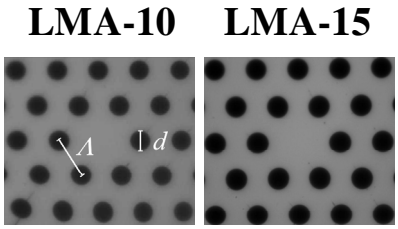

Fig. 1. Optical microscope images of LMA-10 and LMA-15. Remark: not to scale.

The ratio of the hole diameter, d, to the pitch of the structure, Λ, is approximately equal to 0.50 for all the fibers, which ensures single-mode guidance from visible to infrared wavelengths [16]. The large core size of the fibers results in low numerical aperture and, thereby in small divergence of the output beam. The length of LMA-10 and LMA-15 was 100 m whereas LMA-20 was slightly shorter (90 m). The single-mode guidance over a broad wavelength range for the three fibers was verified both theoretically using a beam propagation method [17] and experimentally by launching light at 532 nm into the fibers. The characteristics of the LMA-fibers are summarized in Table 1. The dispersion of each fiber calculated with the beam propagation technique is plotted in Fig. 2(a) as a function of wavelength. As can be expected, the zero-dispersion wavelength is an increasing function of the fiber diameter. The nonlinear coefficient of the fibers was estimated from the mode-field diameter obtained from the beam propagation method. It is interesting to note that the nonlinear coefficient does not scale exactly as the inverse square of the core size. Due to a large effective modal area, the nonlinear coefficient of this type of fiber is much lower than that of narrow-core MFs. Nevertheless, for the purpose of SC generation, the lower nonlinearity can be compensated for by an increase in the fiber length.

Table 1. Characteristics of the fibers. λ_{ZD}: zero-dispersion wavelength, γ: nonlinear coefficient (given at 1064 nm), and NA: numerical aperture (given at 1064 nm).

	LMA-10	**LMA-15**	**LMA-20**
Core size [μm]	10.8	14.8	19.4
Length [m]	100	100	90
λ_{ZD} [nm]	1175	1215	1230
γ [$W^{-1}\cdot km^{-1}$]	3	2.1	1.4
NA	0.1	0.07	0.055

#8283 - $15.00 USD Received 26 July 2005; Revised 14 September 2005; Accepted 11 October 2005

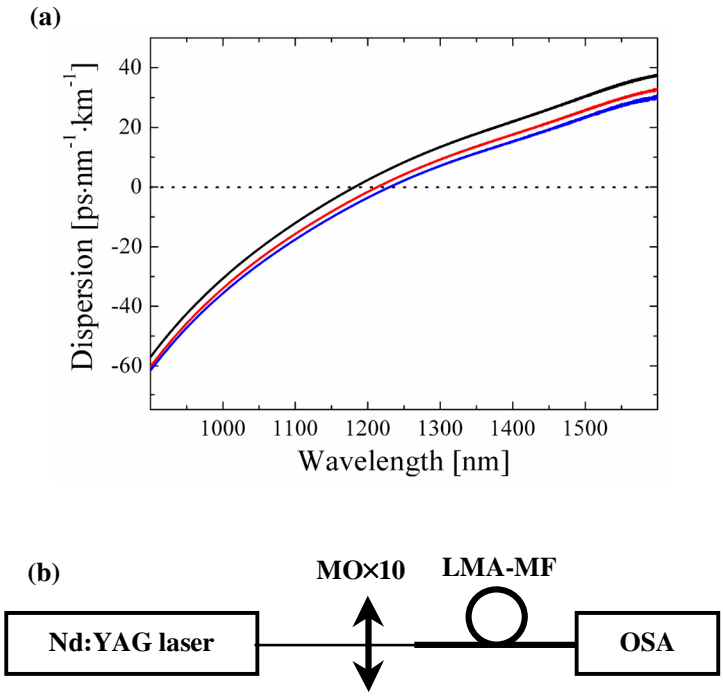

Fig. 2. (a) Dispersion profile of the LMA-MFs. The black, red and blue lines correspond to LMA-10, LMA-15 and LMA-20, respectively. (b) Experimental setup. MO: microscope objective and OSA: optical spectrum analyzer.

A schematic of the experimental setup is illustrated in Fig. 2(b). In order to generate the continuum, the light emitted from a passively Q-switched Nd:YAG laser at the wavelength of 1064 nm was launched into the LMA-MFs. The spectrum and temporal profile of the pulses measured at the output of the laser are plotted in Fig. 3. The laser operates at a repetition rate of 25 kHz and produces pulses with a temporal width of ~3 ns. The maximum average output power of the laser is 180 mW, corresponding to a peak power of ca. 1.7 kW. Note that, for each LMA-MF, the pump wavelength is located in the normal dispersion region. The output of the laser was not polarized and no attempt was made to obtain linear polarization as this would only result in a decrease of available power. Furthermore, accurate characterization of the polarization properties of these fibers showed a small residual birefringence compared to narrow-core MFs [15] and no polarization dependence is therefore expected for the continuum. Coupling to the LMA-MFs was achieved with a simple ×10 microscope objective (Zeiss CP-Achromat ×10). The spectrum at the output of the fibers was monitored with an optical spectrum analyzer (Ando AQ6315B).

#8283 - $15.00 USD Received 26 July 2005; Revised 14 September 2005; Accepted 11 October 2005

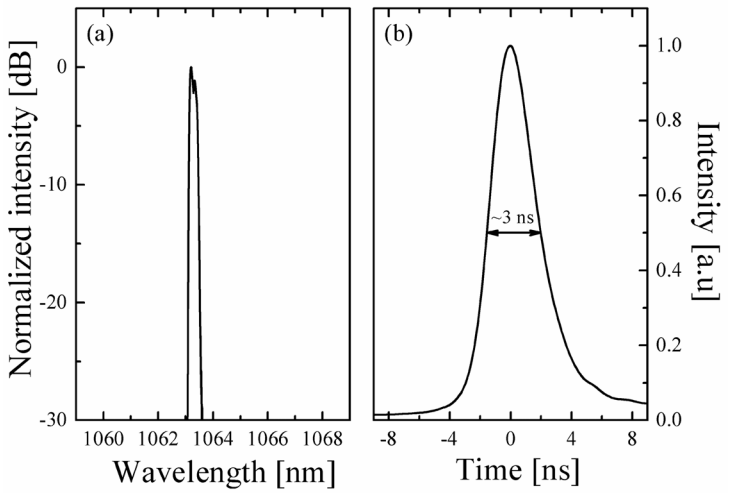

Fig. 3. Spectrum (a) and time trace (b) of the pump pulses. Note the slight offset of the OSA wavelength axis. The resolution of the OSA was set to 0.05 nm.

The supercontinuum spectrum generated in LMA-10 is shown in Fig. 4 for increasing average power. For maximum power coupled into the fiber, the SC spectrum covers more than an optical octave (from 600 nm to beyond 1800 nm) with a relatively good smoothness in the infrared region. Note that despite the length of the fiber, the OH absorption peak at around 1390 nm is rather weak here in contrast to SC generated in narrow-core MFs. This is readily explained by the fact that the OH-losses are strongly enhanced for reduced core diameters. All the spectral components were found to propagate in the fundamental mode. The photograph of the SC output mode observed in the far-field at a wavelength of 630 nm (see inset in Fig. 4) clearly illustrates single-mode propagation. Note that the peak at 800 nm corresponds to the remain of the diode used to pump the Q-switched laser.

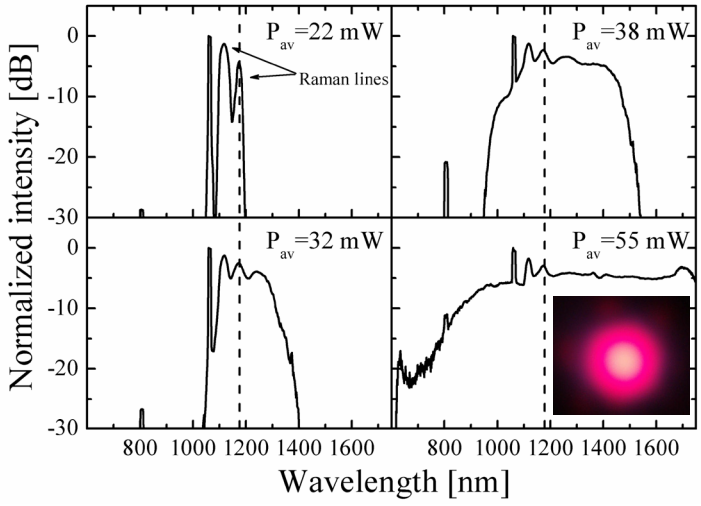

Fig. 4. Supercontinuum generated in LMA-10. P_{av}: avarage power measured at the fiber output. Inset: Output mode at $\lambda \approx 630$ nm (taken with a digital camera). The dashed line marks the location of the zero-dispersion wavelength. The peak at 800 nm corresponds the remain of the diode employed to pump the Nd:YAG crystal. The resolution of the OSA was set to 10 nm.

#8283 - $15.00 USD Received 26 July 2005; Revised 14 September 2005; Accepted 11 October 2005

The physical processes leading to the formation of the continuum spectrum were studied by monitoring the growth of the SC while increasing the input power. We could conclude that the mechanisms leading to the continuum in this case rely primarily on the processes of cascaded stimulated Raman scattering and four-wave mixing. At low input power (P_{av}≈22mW), two Raman lines centered respectively at ~1115 nm and ~1175 nm are observed. The location of the lines agrees well with the 13.2 THz frequency shift induced by Raman scattering. At this stage, no symmetrical broadening typical of four-wave mixing, as is the case for narrow-core MFs, occurs [7-8]. This fact can be explained by the large frequency detuning between the pump wavelength and the location of the zero-dispersion wavelength, preventing the phase-matching condition to be fulfilled. When increasing the input power another Raman line falling into the anomalous dispersion region of the fiber appears in the spectrum at 1241 nm. The position of the line is slightly offset from the theoretical 13.2 THz shift from the previous line at 1175 nm due to four-wave mixing across the zero-dispersion wavelength which shifts the gain peak [18]. The shift is even larger for higher power values (P_{av}≈38 mW) as expected from the four-wave mixing theory. At high power values, this Raman-assisted four-wave mixing line subsequently seeds the formation of short soliton pulses experiencing the soliton-self frequency shift [19-20]. The result is a smooth continuum for wavelengths above the zero-dispersion wavelength. Furthermore, the zero-dispersion wavelength is close enough to the pump so that, for high power values, four-wave mixing can occur between the pump and Stokes lines produced by Raman scattering [21-22]. The coupling between the pump and Stokes frequency components results in the generation of strong anti-Stokes bands that extend the continuum towards blue wavelengths. Preliminary simulations also indicate that cross-phase modulation between the frequency components located in the anomalous dispersion region (in the form of soliton experiencing the soliton self-frequency shift) and those located in the normal dispersion region contribute to the further expand and smooth out the blue part of the SC similarly to what was reported in narrow-core MFs [23].

The experiment was subsequently repeated for LMA-15. The development of the spectrum of the supercontinuum generated in this fiber as a function of average power is illustrated in Fig. 5. At maximum input power the -20 dB bandwidth of the spectrum extends from 1000 nm to 1750 nm. The evolution of the red side of the continuum as a function of power is nearly identical to Fig. 4. However, a substantial decrease appears on the blue side of the spectrum compared to the continuum generated in LMA-10. This decrease can be attributed to two factors, the lower magnitude of the nonlinear coefficient and the larger separation between the pump and the zero-dispersion wavelength, which reduces the efficiency of four-wave mixing processes between the Raman lines and the pump [22]. The latter factor is most likely to play a greater role in the quasi-absence of blue spectral components since the broadening of the spectrum at lower power values is comparable for LMA-10 and LMA-15. The divergence of the infrared output beam was also observed to be less than with the LMA-10 fiber.

#8283 - $15.00 USD Received 26 July 2005; Revised 14 September 2005; Accepted 11 October 2005

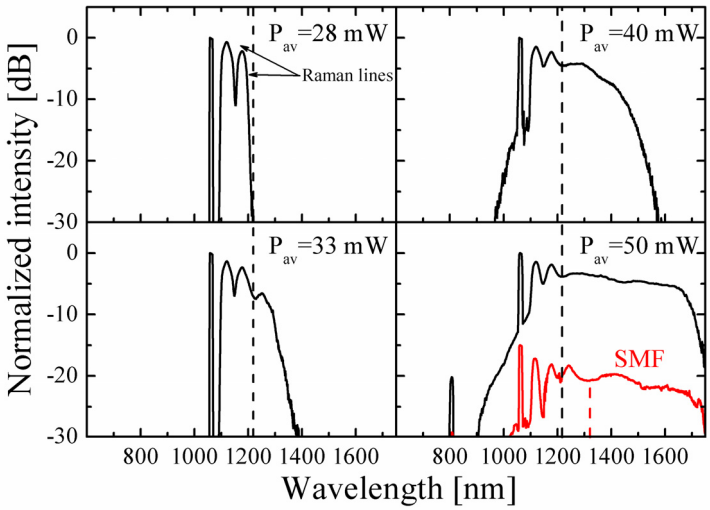

Fig. 5. Spercontinuum generated in LMA-15 and in a standard single-mode fiber (red). P_{av}: avarage power measured at the fiber output. The dashed lines mark the location of the zero-dispersion wavelength. For clarity, an arbitrary offset has been added to the SC spectrum of the standard single-mode fiber. The peak at 800 nm corresponds to the remain of the diode employed to pump the Nd:YAG crystal. The resolution of the OSA was set to 10 nm. SMF: single-mode fiber.

For comparison, we also performed the experiment in a 100 meter-long standard single-mode fiber (Draka NK Cables SMF G.652B), which yielded a supercontinuum whose spectrum is very similar to that generated in LMA-15 as can be seen from the red trace in Fig. 5. Nonetheless, the output of the standard fiber was strongly multi-moded, the divergence of beam much larger than in the previous cases and the spectrum exhibited dips in the OH-absorption bands. Also, a third distinct Raman line appears in the SC spectrum of the single-mode fiber as the zero-dispersion wavelength is located at a longer wavelength compared to LMA-15. Besides, the SC stability was observed to be degraded compared to the LMA-MFs, most likely due to the strong multi-mode behaviour of the standard fiber at the pump wavelength. Therefore, employing LMA-MFs offers advantages over standard single-mode fibers to obtain a smooth, single-mode SC with a low divergence of the output beam. We also point out that, due to the low numerical aperture of the LMA-MFs and relatively large size of the output beam, coupling of the SC light to a standard fiber with high efficiency could be achieved by careful alignment, without any additional optics. This is in contrast to SC generated in narrow-core MFs. Another advantage of LMA-MF is the possibility of direct splicing to a standard fiber without the need for tapers as mode-converters which are used in the case of narrow-core MFs.

Generation of a supercontinuum could not be obtained in LMA-20 as the very low numerical aperture limited the maximum power coupled into the fiber to less than 40 mW using the same microscope objective. This power value is too low to generate a SC as the nonlinearity of LMA-20 is roughly two third that of LMA-15. Nevertheless, the utilization of appropriate optics should yield a broad continuum similar to that obtained with LMA-15 due to the similarity of the dispersion profiles of these two fibers. Indeed, simulations based on a simple model [19] indicate that, with an input power of 80 mW, four Raman lines should be generated along the 90 m fiber, the last one falling into the anomalous dispersion region of LMA-20. Subsequent soliton formation and soliton self-frequency shift should then lead to a continuum spectrum resembling that formed along LMA-15. In our experiments, we were able to observe only the three first Raman lines located at around 1115, 1175 and 1237 nm as shown in Fig. 6. Due to the location of the zero-dispersion wavelength and as is the case with the single-mode fiber, the third Raman lines is generated at 1237 nm which is precisely

#8283 - $15.00 USD Received 26 July 2005; Revised 14 September 2005; Accepted 11 October 2005

located at 13.2 THz from the 1175 nm Raman line. This is in contrast with LMA-10 and LMA-15 where the third Raman lines falls into the anomalous dispersion region and its location is therefore strongly affected by four-wave mixing.

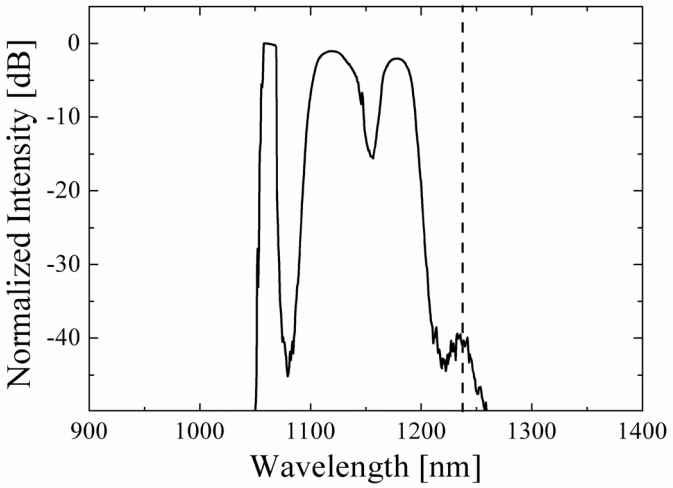

Fig. 6. Raman lines generated in LMA-20. P_{av}=35 mW. The dashed line marks the location of the zero-dispersion wavelength. The resolution of the OSA was set to 10 nm.

An optimized design for a LMA-MF intended for supercontinuum generation depends on several parameters. These include the characteristics of the laser source employed to pump the fiber and the desired bandwidth for the SC (e.g. visible and infrared or solely infrared). In general, if extension of the continuum towards the blue side of the pump is desired, the zero-dispersion wavelength of the fiber should be located near the pump wavelength. With the pump laser used in our experiments, this requires the use of MF with a mode field diameter not larger than ~9 μm. This value corresponds to LMA-10 and is closed to that of standard single-mode fibers, which may prove to be useful for compatibility reasons. On the other hand, if a very low divergence of the output beam or a very high power SC is needed, a MF with larger area may be required. Furthermore, with larger modal area the zero-dispersion wavelength is located further from the pump wavelength (at least with the laser used here) and the energy from the pump is mostly transferred to the red part of the spectrum, which might be of interest for some particular applications. Also, larger mode area usually yields lower OH absorption at 1390 nm. As a consequence, the magnitude of the dip observed around this wavelength in the SC spectrum is reduced for larger fiber core dimensions (~0.9/0.5 dB for LMA-10/15, respectively), which is in contrast to what has been observed usually with narrow-core MFs.

3. Conclusion

In conclusion, we have demonstrated supercontinuum generation in large mode-area microstructured fibers. The supercontinuum bandwidth depends on the dispersion profile and modal area of the fundamental mode. More than an octave-spanning continuum was obtained in a 10 μm core MF. All the spectral components of the continuum generated in the LMA-MFs were found to propagate in the fundamental mode of the fiber. This type of source could be very attractive for applications requiring very low divergence of the output beam. Finally, the large area of the fibers should allow for the generation of extremely high power supercontinuum as the damage threshold is in this case considerably increased. As the attenuation in LMA-MFs is still low at long wavelengths, larger power should result in continuum extending substantially beyond 2000 nm.

#8283 - $15.00 USD Received 26 July 2005; Revised 14 September 2005; Accepted 11 October 2005

Acknowledgments

This work has been carried out within the project entitled “Photonic crystal based integrated optics” of the Future Electronics research program financed by the Academy of Finland (Project No: 205481). The graduate school of Modern Optics and Photonics is also acknowledged for financial support. We are also grateful to S. C. Buchter for the generous loan of the pump source. Crystal Fibre A/S is acknowledged for kindly providing the fiber samples.

#8283 - $15.00 USD Received 26 July 2005; Revised 14 September 2005; Accepted 11 October 2005